Research Article 2018, **3**(6), 419-424 Advanced Materials Proceedings

Enhancement of luminescence properties of Mn^{2+} substituted dysprosium doped Zinc sulfide nanophosphor

S. Rajesh[1]*, K. Thyagarajan[2], Vasudeva Reddy Minnam Reddy[3]

[1]*Department of Physics, JNTUA College of Engineering, Pulivendula-516390, India.*
[2]*Department of Physics. JNTUA College of Engineering, Pulivendula-516390, India.*
[3]*School of Chemical Engineering, Yeungnam University, 280 Daehak-ro, Gyeongsan 38541, South Korea*

*Corresponding author

DOI: 10.5185/amp.2018/412
www.vbripress.com/amp

Abstract

Zinc Sulfide nanophosphor (ZnS) nanophosphor doped with 2 mol % Dysprosium (Dy) and co-doped with (2 – 6) mol % Manganese (Mn) was successfully prepared by cost-effective chemical co-precipitation method using polyvinylpyrrolidone (PVP) as the capping agent. The effects of dopant and co-dopant concentrations on the various properties of ZnS were investigated by various characterizations like Powder X-ray Diffraction (*PXRD)* studies confirmed the cubic zinc blende structure of ZnS and no impurity peaks corresponding to Dy doping and Co-doped by Mn was observed. Scanning Electron Microscope (*SEM*), Energy Dispersive X-ray spectroscopy (*EDAX*) confirmed the presence of dopant Dy and co-dopants Mn in the prepared ZnS. Photoluminescence (*PL*) studies on Dy doped Mn and co-doped ZnS nanophosphor indicated that the emission wavelength 605 nm is tunable in the range of 400–650 nm with the incorporation of doped Dy and Co-doped Mn into ZnS host lattice with the excitation wavelength of 320 nm. Blue color of ZnS doped Dy by enhances to orange color due to co-doped with Mn ions. The chromaticity co-ordinates *(CIE)* and Correlated color temperature *(CCT)* of the phosphor were shows enhancement of blue to orange region; hence, it is useful for the fabrication of orange component of WLEDs and display applications. Copyright © 2018 VBRI Press.

Keywords: Powder X-ray diffraction, capping agent, co-precipitation, scanning electron microscopy, photoluminescence.

Introduction

Nanoparticles have been very much attracted the researchers in the field as the transition from micro particles to nanoparticles was seen to lead to huge changes in the physical and chemical properties of a material. Nano-sized materials with uniform morphology have received great interest due to their importance in basic scientific research and potential knowledge applications. Due to their small size, nanoparticles exhibit novel material properties that are significantly different from those of their bulk counterparts. Because of these physical properties they find many potential applications in areas such as nonlinear optics, photoluminescence, electronics, catalysis, solar cells and optoelectronics and soon [1- 6].

Semiconductor nanoparticles are themselves highly unstable, and in the absence of capping agent, they agglomerate very rapidly. For this reason bonding of capping agents to nanoparticles is necessary to provide chemical passivation and also to improve the surface state which has substantial influence on the optical and electronic properties of nanoparticles. Luminescence properties of Zinc Sulfide nanophosphor (ZnS) can be controlled using various dopants such as Ni, Fe, Mn, Cu etc. Various transition metal ions and rare-earth ions as impurities doped in nanocrystalline ZnS host, such as Cu^{2+}, Mn^{2+}, Pb^{2+}, Ni^{2+}, Cd^{2+}, Co^{2+}, Eu^{3+}, Sm^{3+}, Tb^{3+}, Er^{3+} etc. not only give luminescence in various regions but also can add to the excellent properties of ZnS [7]. In the present study reports the preparation of pure ZnS, 2 mol % Dysprosium (Dy^{3+}) doped and (2 - 6) mol % of Manganese (Mn^{2+}) co-doped into ZnS host lattice by using simple and cost-effective chemical co-precipitation method. The effect of dopant and co-dopant concentration on various properties of ZnS was studied. The prepared samples were well characterized by Powder X-ray diffraction (PXRD), scanning electron microscopy (SEM) and Energy Dispersive X-ray Analysis (EDAX). Photoluminescence (PL) studies were made at RT and discussed in detail.

Experimental

Preparation of pure, 2 mol % doped Dy^{3+} and (2-6) mol % Mn^{2+} co-doped ZnS nanophosphor

All the chemicals were of A.R. (Analytical Reagent) grade and were used without any further purification. The pure, 2 mol % Dy^{3+}doped and (2 - 6) mol % Mn^{2+} co-doped ZnS nanophosphor was prepared by co-precipitation method using pure zinc acetate, Dysprosium chloride hexahydrate, Manganese acetate (Tetra hydrate) and Sodium sulfide [8]. The calculated amounts of $Zn(CH_3COO)_2$, $Cl_3Dy.6H_2O$ and $(CH_3COO)_2Mn.4H_2O$ were dissolved in 100 ml of deionized water. For this solution 50 ml of Sodium sulfide solution is added drop wise under constant stirring until to get fine precipitate of 2 mol % of Dy^{3+} doped and (2 - 6) mol % of Mn^{2+} co-doped ZnS nanophosphor. After the completion of the reaction, the resultant white precipitate was centrifuged and products were collected, thoroughly washed with deionized water and ethanol for several times and dried. The flow chart of complete process and the steps involved in the preparation of 2 mol % of Dy^{3+} doped and (2 - 6) mol % of Mn^{2+} co-doped ZnS nanophosphor was shown in **Fig. 1** and were subjected to various characterization and photoluminescence studies.

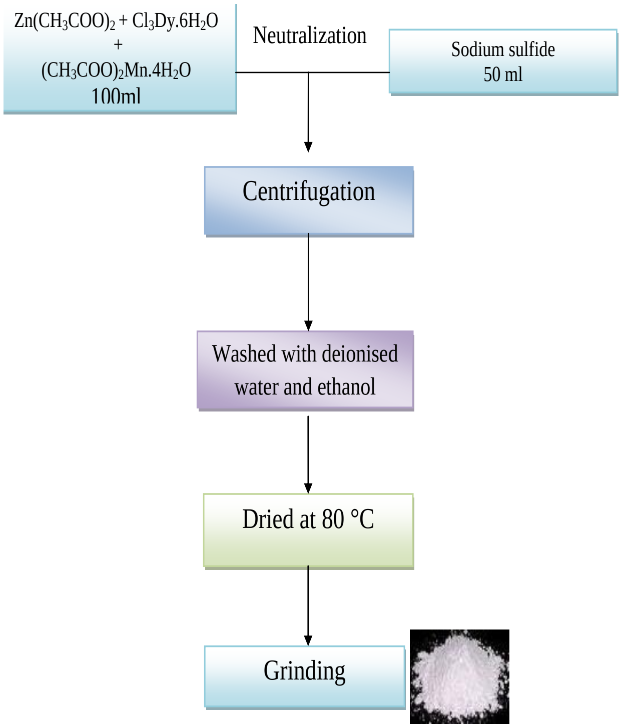

Fig. 1. Flow chart showing step involved in co-precipitation method of Pure, 2 mol % Dy doped and 2 mol % Dy doped with (2 – 6) mol % Mn co-doped ZnS nanophosphor.

Characterization

The PXRD patterns of the samples were collected on a Seifert 3003 TT X-Ray Diffractometer with the Cu K$_\alpha$ radiation (λ=1.5405A°). Morphological studies and elemental compositions for the prepared samples were analyzed through EDAX using Oxford Inca Penta FeTX3 EDS instrument attached to Carl Zeiss EVO MA 15 SEM. PL spectra of the present nanophosphor have been recorded using a Horiba-Fluorolog-3 (Model FL3-22) Spectroflourimeter at RT.

Results and discussion

Powder X-ray diffraction

The PXRD patterns of the pure, doped and co-doped nanophosphors show a single-phase with cubic zinc blende structure with three diffraction peaks corresponding to (111), (220) and (311) diffraction planes of cubic zinc blende structure as per the standard JCPDS No. 80-0020. No secondary phase was detected indicating that Dy doped and co-doped Mn is incorporated into the ZnS host lattice. The broadened of PXRD peaks indicate that the nanocrystalline nature of the prepared samples. The average crystallite size was obtained from the most prominent PXRD peak, (111) using Debye-Scherrer's formula [8, 9].

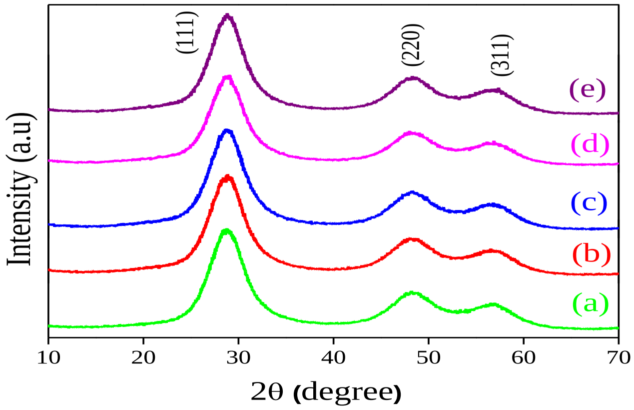

Fig. 2. XRD spectra of (a) Pure (b) 2 mol % Dy doped (c-e) 2 mol % Dy doped with (2 – 6) mol % Mn co-doped ZnS nanophosphor.

$$d = \frac{k\lambda}{\beta\cos\theta} \tag{1}$$

where, d is the average particle size, k is a content lies between (0.88 - 0.92), the average value taken as 0.9 in the calculation, λ is wavelength of Cu-K$_\alpha$ irradiation (λ = 1.5481 A°), β is the full width at half maximum intensity of the diffraction peak and θ is the diffraction angle. The particle size of the prepared samples is ~ 2 nm. The PXRD spectra of pure, 2 mol % of doped Dy and (2 – 6) mol % Mn co-doped ZnS nanophosphor are shown in **Fig. 2.**

Further, effective particle size and strain present in the pure, 2 mol % of Dy doped and (2 – 6) mol % Mn co-doped ZnS nanophosphor was estimated using the W-H equation.

$$\beta\cos\theta = \frac{k\lambda}{D} + 4\varepsilon\sin\theta \tag{2}$$

where 'ε' is the strain associated with the nanoparticles [10]. The above equation represents a straight line plotting the graph of 'β cosθ' verses '4sinθ'. The effective particle size for which the lattice strain has been taken into account can be estimated from the extrapolation of the plot as shown in **Fig. 3.** From the W-H plots the lattice strain is extracted from the slope and the crystalline size was extracted from the y-intercept of the linear fit [11]. The average crystallite size was found to be ~ 2 nm and well matched with the Scherrer's formula. Lattice strain of pure, 2 mol % Dy doped ZnS is 6.34 × 10^{-3} and 6.58 × 10^{-3} respectively are almost same. But due to co-dopant Mn concentration increases from (2 – 6) mol % strain is also increases shown in the **Table. 1.**

Table. 1. Estimated structural parameter of (a) Pure (b) 2 mol % Dy doped and (c-e) 2 mol % Dy doped with (2 – 6) mol % Mn co-doped ZnS nanophosphor.

Average Crystallite Site	Pure ZnS	2 mol % Dy doped ZnS	2 mol % Dy doped and (2 – 6) mol % Mn co-doped ZnS		
			2 mol %	4 mol%	6 mol %
Scherer's equation. in nm.	1.61	1.62	1.50	1.55	1.45
W-H Plot. in nm.	1.62	1.65	2.36	2.43	2.62
Lattice strain ϵ x10^{-3}	6.34	6.58	23.65	23.04	29.75

Morphological studies

The surface morphology is studied by a SEM, especially by observing the top and cross-sectional views of the sample. The surface morphologies of the pure, Dy (2 mol %) doped and Mn (2 – 6) mol % co-doped ZnS nanophosphor were shown in **Fig 3 (a - e)** respectively. All the samples were highly pores and agglomerated. It is noticed that in the doped samples the agglomerated particles were appear and agglomeration decreased with increasing co-dopant Mn concentration up to 4 mol % thereafter it increases and it shows in nano size.

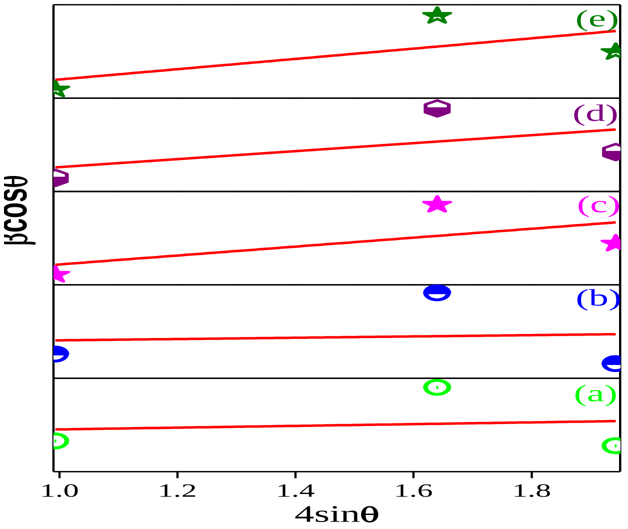

Fig. 3. W-H Plots of (a) Pure (b) 2 mol % Dy doped (c) 2 mol % Dy doped and (c-e) 2 mol % Dy doped with (2 – 6) mol % Mn co-doped ZnS nanophosphor.

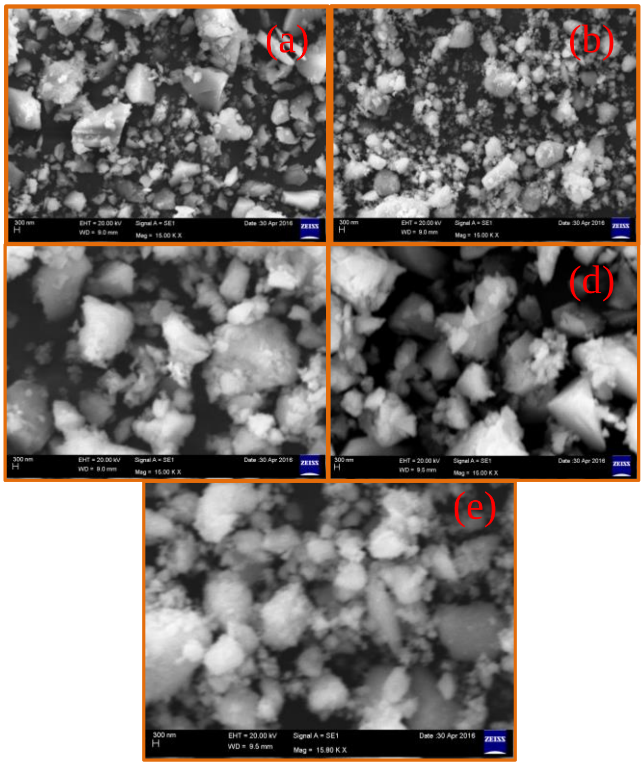

Fig. 4. SEM pictures of (a) Pure (b) 2 mol % Dy doped (c) 2 mol % Dy doped and (c-e) 2 mol % Dy doped with (2 – 6) mol % Mn co-doped ZnS nanophosphor.

Elemental analysis

Chemical composition analysis of all the prepared nanophosphor was done by EDAX technique. In order to analyze the amount of pure, Dy (2 mol %) doped and Mn (2 – 6) mol % co-doped ZnS nanophosphor content and distribution in ZnS this technique is much useful. **Fig. 4 (a - e)** shows EDAX spectra of pure, 2 mol % Dy doped and (2 – 6) mol % Mn co-doped ZnS nanophosphor respectively with the atomic weight % in the inset tables. EDAX spectra of the samples confirmed that the amount of Zn, S, Dy and Mn were close to the nominal (target) values. This confirms the effective doping Dy and co-doping of Mn into ZnS host lattice matrix.

Photoluminescence (PL) studies

The PL Excitation spectra of pure, Dy (2 mol %) doped and 4 mol % Mn co-doped ZnS nanophosphor were shown in **Fig 5.** The intense and common to pure, Dy (2 mol %) doped and 4 mol % Mn co-doped ZnS nanophosphor excitation peaks shows at 320 nm with other excitation peaks 335, 372, 378 and 388 nm. The entire (2–6) mol % Mn co-doped with ZnS:Dy nanophosphors were excited at a wavelength of 320 nm and the luminescence peak of pure, 2 mol % Dy doped and 4 mol % Mn co-doped ZnS nanophosphor was observed at 605 nm. Compared to pure Zns, (2 mol %) Mn doped ZnS sample showed decreased luminescence intensity due to the reduction of defect sites in the ZnS host lattice [12]. The more intense emission peak

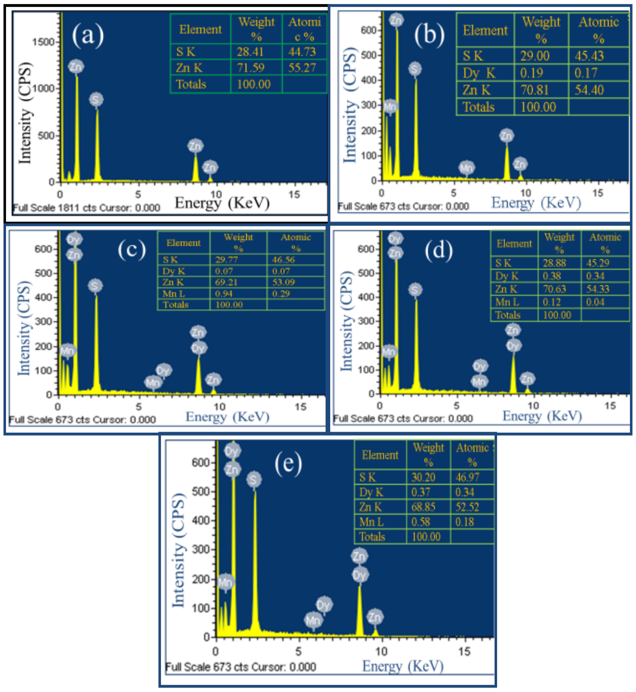

Element	Weight %	Atomic %
S K	28.41	44.73
Zn K	71.59	55.27
Totals	100.00	

Element	Weight %	Atomic %
S K	29.00	45.43
Dy K	0.19	0.17
Zn K	70.81	54.40
Totals	100.00	

Element	Weight %	Atomic %
S K	29.77	46.56
Dy K	0.07	0.07
Zn K	69.21	53.09
Mn L	0.94	0.29
Totals	100.00	

Element	Weight %	Atomic %
S K	28.88	45.29
Dy K	0.38	0.34
Zn K	70.63	54.33
Mn L	0.12	0.04
Totals	100.00	

Element	Weight %	Atomic %
S K	30.20	46.97
Dy K	0.37	0.34
Zn K	68.85	52.52
Mn L	0.58	0.18
Totals	100.00	

Fig. 5. EDAX spectra of (a) Pure (b) 2 mol % Dy doped and (c-e) 2 mol % Dy doped with (2 – 6) mol % Mn co-doped ZnS nanophosphor. (Inset: table shows % of atomic weights).

observed at around 428 nm and weak intense emission at 498 nm is attributed to the transition from excited ${}^4T_1 \rightarrow {}^6A_1$ of Dy ions. Incorporation of Dy ions into the ZnS host lattice and substitution of host cation sites, the mixing between the s and p electrons of the host ZnS and the d electrons of Dy occurred and made the forbidden transition of ${}^4T_1 \rightarrow {}^6A_1$ partially allowed, leads to the characteristic emission of DY indicating that the successful incorporation of Dy ions into the ZnS host lattice matrix [13-15].

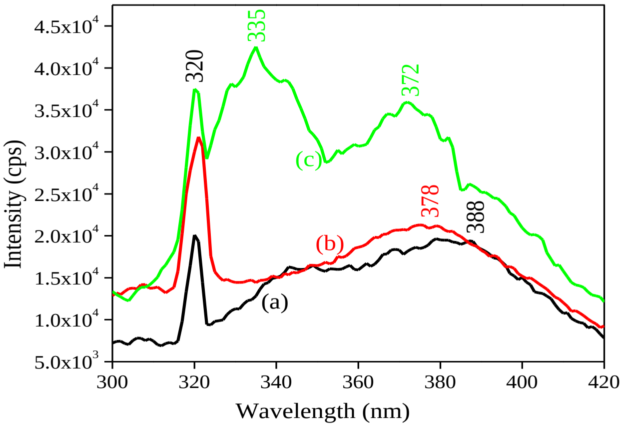

Fig. 6. Excitation spectra of (a) Pure (b) 2 mol % Dy doped and (c) 2 mol % Dy doped with 4 mol % Mn co-doped ZnS nanophosphor.

It is clearly observed that the incorporation of Mn into ZnS:Dy enhances the luminescence peak intensity there after it was decreases by increase of Mn concentration. This may be due to the cross-linking centers provided by Mn in the ZnS:Dy matrix. The luminescence intensity of doped Dy and co-doped Mn into ZnS nanophosphor was about 7 times more that of the Dy doped ZnS nanophosphor. It was evident from the **Fig. 8** that PL intensity increases with increase in Mn co-dopant concentration up to 4 mol % and thereafter it decrease with further increase in Mn co-dopant concentration. The decrease in PL intensity could be explained by the phenomenon of concentration quenching. Initially, the PL intensity increases with increase in Mn concentration because the ionic radius of Mn (0.81 Å) was slightly lesser than Dy (1.05 Å) and Zn (0.88 Å), therefore a small percentage of impurity ions can only accommodate in the ZnS host matrix. Further, with increase in the Mn concentration the charge imbalance may occur as a consequence, trapping centres were created. This trapping centres results in cross relaxation and non-radiative transition which causes concentration quenching [16-18].

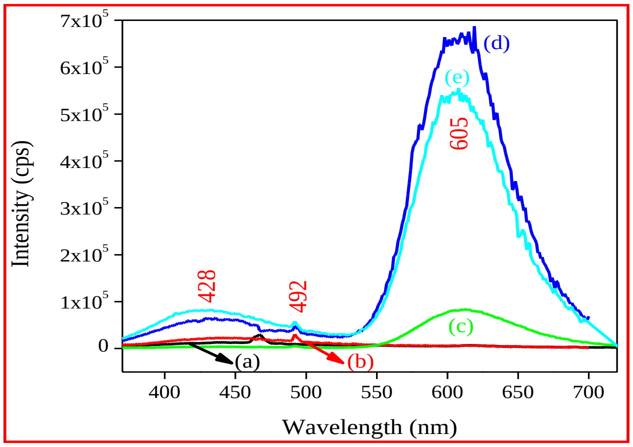

Fig. 7. Emission spectra of (a) Pure (b) 2 mol % Dy doped and (c-e) 2 mol % Dy doped with (2 – 6) mol % Mn co-doped ZnS nanophosphor.

Non-radiative energy transfer distance (R_c) can be estimated by using the relation proposed by Blasse [19].

$$R_c = 2\left[\frac{3V}{4\pi X_c N}\right]^{1/3} \tag{3}$$

where, V was the unit cell volume, X_c was the critical concentration of the Mn ion, N was the number of host cations in the unit cell. For ZnS:Dy:Mn nanophosphor material V= 397.67 Å^3, N = 6 and X_c = 0.04. Hence the obtained non-radiative energy transfer distance was 12.18 Å.

According to Blasse the non-radiative energy transfer between Mn ions can take place by radiative re-absorption, exchange interaction or multipolar interaction. Radiative re-absorption dominates when there was a broad overlap of sensitizer and activator spectra which was unlikely to be occurring in this case. The exchange interaction occurs when the critical energy transfer distance was less than 5 Å which was far less than the calculated R_c value of ZnS:Dy:Mn nanophosphor. Since the critical distance between Mn ions was greater than

5 Å, only multipolar interaction exists which the main cause for concentration quenching. The emission mechanism of Mn in ZnS:Dy nanophosphors can be proposed as follows. The emission intensity (I) per activator ion follows the equation [20].

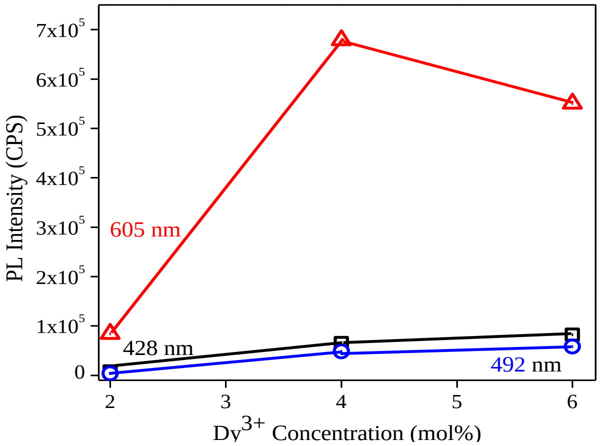

Fig. 8. The variation of PL intensity with different Mn concentration.

$$\frac{I}{X} = k\left[1+\beta(x)^{\theta/3}\right]^{-1} \tag{4}$$

where, x was the activator concentration, I/x was the emission intensity (I) per activator ion, k and β were constants for a given host under the same excitation condition. According to equation 4, θ = 3 for the energy transfer among the nearest – neighbor ions (exchange interaction), while θ = 6, 8 and 10 for dipole-dipole (d-d), dipole- quadrupole (d-q) quadrupole – quadrupole (q-q) interaction respectively. Assuming that $\beta(x)^{\theta/3} >> 1$, equation 4 can be specified as follows:

$$\log\frac{I}{X} = k^1 - \frac{\theta}{3\log x} \tag{5}$$

From the slope of Equation 5, the electric multipolar character (θ) can be obtained by the slope (−θ/3) of the plot log (I/x) vs log x. It was observed from the **Fig. 9** that the dependence of log (I/x) on log x was linear and the slope was −1.722. Thus, the value of θ can be calculated as 5.166 which were approximately equal to 6, which means that the d–d interaction was the main mechanism for the concentration quenching in the Mn co-doped ZnS:Dy nanophosphor.

The color co-ordinates of ZnS:Dy:Mn (2 - 6 mol %) were calculated based on the Commission International de I'Eclairage (CIE) 1931 standard. The chromaticity coordinates of pure, 2 mol % Dy doped ZnS located in Blue region and (2 – 6) mol % Mn co-doped ZnS nanophosphor enhances the emission wavelength to orange region shown in star mark in **Fig. 10**. All the co-doped samples were located in orange region shown in the star mark. This indicates that the present phosphor was highly useful for the fabrication of orange component of white light. The luminescent color coordinate values (x, y) obtained were given in inset table of **Fig. 10.**

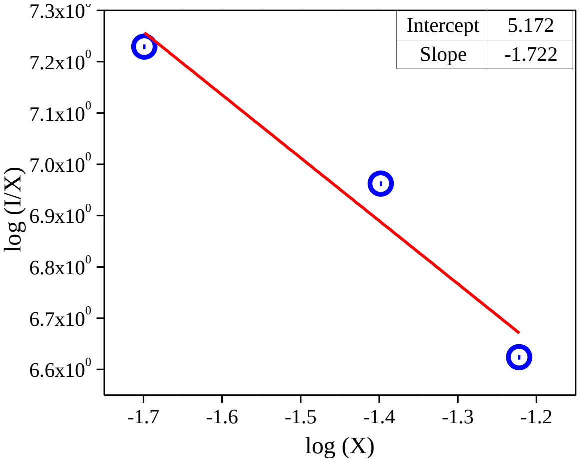

Fig. 9. Relation between log (x) vs log (I/x) in ZnS:Dy:Mn nanophosphor.

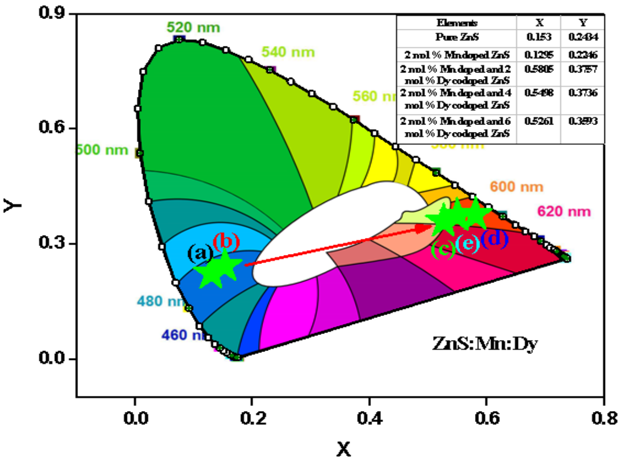

Elements	X	Y
Pure ZnS	0.153	0.2434
2 mol % Mn doped ZnS	0.1295	0.2346
2 mol % Mn doped and 2 mol % Dy codoped ZnS	0.5805	0.3757
2 mol % Mn doped and 4 mol % Dy codoped ZnS	0.5498	0.3736
2 mol % Mn doped and 6 mol % Dy codoped ZnS	0.5261	0.3593

Fig. 10. CIE chromaticity diagram of (a) Pure (b) 2 mol % Dy doped and (c-e) 2 mol % Dy doped and (2 - 6) mol % Mn co-doped ZnS nanoparticles. (Inset: table shows x and y values).

Correlated color temperature (CCT) can be estimated by Planckian locus, which is only a small portion of the (x, y) chromaticity diagram and there exist many operating points outside the Planckian locus. If the coordinates of a light source do not fall on the Planckian locus, the CCT is used to define the color temperature of a light source. CCT is calculated by transforming the (x, y) coordinates of the light source to (U′, V′) by using following equations, and by determining the temperature of the closest point of the Planckian locus to the light source on the (U′, V′) uniform chromaticity diagram shown in **Fig. 11** (Inset: table shows U′, V′ and CCT values) [21].

$$U' = \frac{4x}{-2x+12y+3} \tag{6}$$

$$V' = \frac{9y}{-2x+12y+3} \tag{7}$$

Also, average CCT was found to be 1864 K. Therefore, the present phosphor was enchance the blue to orange region of ZnS:Dy:Mn nanophosphor and hence, it is highly useful for the production of artificial white light to be similar to those of natural white light owing to its better spectral overlap in WLEDs and in display applications.

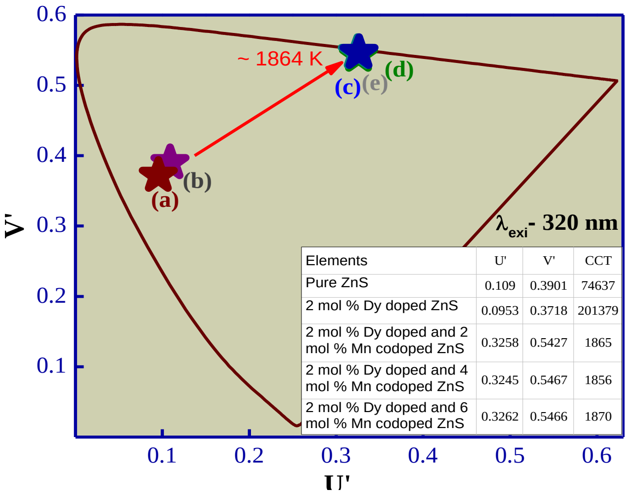

Elements	U'	V'	CCT
Pure ZnS	0.109	0.3901	74637
2 mol % Dy doped ZnS	0.0953	0.3718	201379
2 mol % Dy doped and 2 mol % Mn codoped ZnS	0.3258	0.5427	1865
2 mol % Dy doped and 4 mol % Mn codoped ZnS	0.3245	0.5467	1856
2 mol % Dy doped and 6 mol % Mn codoped ZnS	0.3262	0.5466	1870

Fig. 11. CCT diagrams of (a) Pure (b) 2 mol % Dy doped and (c-e) 2 mol % Dy doped and (2 - 6) mol % Mn co-doped ZnS nanoparticles. (Inset: table shows U′, V′and CCT values).

Conclusion

Pure, 2 mol % Dy doped, (2 – 6) mol % Mn co-doped ZnS nanophosphor were successfully synthesized by facile chemical co-precipitation technique at RT. PXRD studies showed the cubic zinc blende structure of the prepared samples and the broadened peaks in the X-ray diffractograms indicates the nanocrystalline nature of the prepared samples. SEM analysis attached with EDAX reveals the surface morphology and effective incorporation of Dy dopants and (2 – 6) mol % Mn co-dopants into ZnS host lattice. SEM images showed slight decrease in agglomeration with increasing Mn concentration. PL emission peaks of prepared samples were observed at 605 nm and the luminescence intensity is enhanced with increasing Mn co-dopant concentration. The CIE and CCT chromaticity co-ordinates situated in the orange region, hence the prepared phosphor enhances the blue region to orange region due to Mn co-doped with ZnS:Dy nanophosphor. Hence prepared phosphor might be useful in orange component of WLED’s and solid state display applications.

Acknowledgements

The author Dr. K. Thyagarajan sincerely thanks the Principal and Management of TEQIP-2 JNTUCEP, Pulivendula, for providing the necessary amenities for the work. The author S. Rajesh would like to thank Prof. C.K. Jayasankar, [MoU-DAE-BRNS Project (No.2006/34/36/BRNS/3174)], Department of Physics, S.V. University, Tirupathi, India for providing lab facilities.

References

1. P.V. Kamat, D. Meisel, Eds. Semiconductor Nanoclusters, Studies in Surface Science and Catalysis, Elsevier, Amsterdam (1996) 103.
2. H. Weller, Angew Chem. Int. Ed Engl., 32 (1993) 41.
3. X. Fang, T. Zhai, U.K. Gautam, L. Li, L. Wu, Y. Bando, D. Golberg, Prog. Mater. Sci., 56 (2011) 175.
4. M. Bredol, J. Merikhi, J. Mater. Sci., 33 (1998) 471.
5. J. Leeb, V. Gebhardt, G. Muller, D. Haarer, D. Su, M. Giersig, G. McMahon, L. Spanhel, J. Phys. Chem. B, 103 (1999) 7839.
6. W. Chen, Z. Wang, Z. Lin, L. Lin, Appl. Phys. Lett., 70 (1997) 1465.
7. W. Q. Peng, G. W. Cong, S. C. Qu, and Z. G. Wang, 29 (2006) 313.
8. S. Wei, B. I. Lee, Z. Lin, W. Tong, B. K. Wagner, W. Park, and C. J. Summers, 92 (2001) 73–78.
9. B. D. Cullity, Elements of X-ray Diffraction, second ed. (Addison-Wesley Company, USA, (1978) 102.
10. P. Klug, L.E. Alexander, In: X-ray Diffraction Procedure, Wiley, New York, 1954.
11. G.K. Williamson, W.H. Hall, Acta Metall. **1** (1953) 22.
12. R. Kumar, R. N. Baghel, V. K. Chandra, and B. P. Chandra, Superlattices Microstruct., 86 (2015) 256.
13. B. Dong, L. Cao, G. Su, W. Liu, H. Qu, D. Jiang, J. Colloid and Interface Science, 339 (2009) 78.
14. S. Biswas, S. Kar, S. Chaudhuri, J. Phys. Chem. B, 109 (2005) 17526.
15. S. Ummartyotin, N. Bunnak, J. Juntaro, M. Sain, and H. Manuspiya, Solid State Sci., 14-3 (2012) 299.
16. B. Xia, I.W. Lenggoro, K. Okuyama, Chem. Mater. 14 (2002) 4969.
17. H. Hu, W.H. Zhang, Opt. Mater. 28 (2006) 536.
18. B. M. Manohara, H. Nagabhushana, D.V. Sunitha, K. Thyagarajan, B. Daruka Prasad, S. C. Sharma, B. M. Nagabhushana and R. P. S. Chakradhar, J. Alloys Compd., 592-3 (2014) 319–327.
19. G. Blasse, Philips Res. Rep. 24 (1969) 131-144.
20. L.G Van Uitert. J. Electrochem. Soc. 114 (1967)1048-1053.
21. B.M. Manohara, H. Nagabhushana, K. Thyagarajan, B.D. Prasad, S.C. Prashantha, S.C. Sharma and B.M. Nagabhushana, J. Lumin., 161 (2015) 247.